CORE
Metadata, citation and similar papers at core.ac.uk
Provided by Lehigh University: Lehigh Preserve

Lehigh University
Lehigh Preserve

ATLSS Reports | Civil and Environmental Engineering

9-11-1989

Selection Theory for Part Dimensions, Tolerances, and Equipment Precision: A Prelude to Automated Construction Systems

C. Doydum

N. D. Perreira

Follow this and additional works at: http://preserve.lehigh.edu/engr-civil-environmental-atlss-reports

Recommended Citation

Doydum, C. and Perreira, N. D., "Selection Theory for Part Dimensions, Tolerances, and Equipment Precision: A Prelude to Automated Construction Systems" (1989). ATLSS Reports. ATLSS report number 89-14:.
http://preserve.lehigh.edu/engr-civil-environmental-atlss-reports/153

This Technical Report is brought to you for free and open access by the Civil and Environmental Engineering at Lehigh Preserve. It has been accepted for inclusion in ATLSS Reports by an authorized administrator of Lehigh Preserve. For more information, please contact preserve@lehigh.edu.

ADVANCED TECHNOLOGY FOR
LARGE
STRUCTURAL SYSTEMS

Lehigh University

Selection Theory for Part Dimensions, Tolerances, and Equipment Precision: A Prelude to Automated Construction Systems

by

C. Doydum

N. D. Perreira

ATLSS Report No. 89-14

September 1989

An NSF Sponsored Engineering Research Center

FOREWORD

Dimensions and tolerances selected during the design stage of a construction project greatly influence the material and fabrication costs, the required performance of the construction equipment, and the quality of fabricated and erected systems. An objective of the Automated Construction Systems project at the NSF Engineering Research Center for Advanced Technology for Large Structural Systems, ATLSS, is to design, build and test cost-effective automated construction systems.

This paper reports the development of a function, the Probability of Successful Assembly (PSA), which relates the ability to erect or assemble components to their dimensions and tolerances and the precision of the equipment used. Non-dimensional tolerances and precisions are used to provide a means to present graphically the underlining relationships in a useful yet general form. In situations where the equipment precision is given a priori-ty, Maximum Allowable Size Ratio (MASR) tables provide a method for determining the part dimensions and tolerances that will lead to various levels of success. The PSA function can be used within a component design, fabrication and erection cost model to determine the size and dimensions of the components and the precision of the equipment required. (In this paper, the PSA function and the MASR tables are restricted to rigid (non-deforming) components; subsequent work will remove this constraint.)

Of particular interest at the ATLSS Center is the adaptation of the PSA function to automated connections in steel, concrete, and composite construction. This paper lays the fundamental theory appropriate to this application.

Cemal Doydum

Research Assistant

Industrial Engineering

N. Duke Perreira

Associate Professor

Mechanical Engineering and Mechanics

INTRODUCTION

The events leading to successful material removal and assembly processes include alignment and processing. Detailed characteristics of these events are governed by the actual geometry and clearance between the mating parts, the initial position and angular alignment of the parts, and by the contact forces between the parts as they are mated. Misalignment may occur prior to, during and after the process. We are concerned with the alignment prior to the process for it is a primary influence on the fate of the remaining sequence.

In an ideal automated assembly of two loosely fitting parts it is desired that the parts are fabricated to their design dimensions with zero tolerance, the clearance between the parts during the insertion process is distributed between the parts in such a way that no collisions or rubbing could occur and the size of the clearance is sufficient to provide the intended function of the assembly. In real automated assembly systems this ideal condition is never met. The precision of the manipulating equipment and fixturing and the fabrication tolerances of the parts being assembled will always be less than perfect. This results in collision and rubbing of the parts during the assembly, the need for intervention, productivity losses and generation of material scrap.

To remedy this situation various techniques have been developed. In automated assembly, the manipulator may be equipped with the ability to sense collisions. Upon the failure of the insertion, error recovery strategies may include a second assembly attempt. Other optimal number of assembly attempts may exist [1]. Such methods may increase the probability of catastrophic failure and the cost of the system while reducing the productivity of the process. In many cases to maximize productivity while minimizing the unit cost it is important that the process be accomplished in the first attempt.

Other solution techniques applicable to assembly processes include the use of chamfers and compliance [2,3]. This has led to the investigation of various chamfer shapes in order to determine the chamfer shape that would create minimum reaction to insertion forces [4,5]. In order to increase the compliance of a manipulator holding a peg compliant devices are placed between the peg and the manipulator [6,7]. A Remote Center Compliance (RCC) device was developed as a simple and cheap solution to achieve the desired compliance [7]. An Instrumented RCC with positional sensors is used to monitor the displacement of the remote center compliances [8]. The monitored displacements could be used by the robot controller to actively correct the relative position of the peg to the hole. An alternative method to this active correction scheme, as presented in this paper, is to design the peg and hole geometry and tolerances and select part manipulation and fixturing devices so that the possibility of poor insertion is reduced.

In some assemblies chamfers cannot be used or they can not be made large enough to guarantee successful insertion without degrading the required function of the assembly. For example, precision machinery must be assembled in a clean environment without generating dust. Burrs and particles generated by rubbing during insertion reduces the reliability of the assembled device [9]. Chamfers can not be used in surface assemblies [10] such as sticking a stamp on an envelope or placement of surface mounted devices onto printed circuit boards.

Surface assemblies are one of a number of the more general cases where alignment errors occur. The alignment problem occurs in all material removal processes where a cutting edge or beam is placed on or against a material. The cutting edge will have a position and size tolerance as it is moved along a desired countour which also has position and size tolerance. A similar alignment error problem occurs in all material combining processes such as laser sintering [11]. A complete understanding of the interaction among the equipment precision and beam dimensions and tolerances is indispensable for the performance improvement of these and similar processes.

The alignment problem has been previously considered by many researchers [12,13,14,15,16]. In these studies, the assembly process performance has been expressed as a function of the nominal part tolerances, equipment precision and the clearance that exists between the parts. This approach does not lend itself to the development of generic alignment performance models which are functions of the non-dimensional tolerances, precision and size ratio variables. The concept of size ratio together with the non-dimensional tolerance and precision plays a central role in the development of the proposed theory.

In this development we present the method as if it were only to be used for the alignment stage of assembly processes. The presentation does not limit the method's use in other forms of the alignment problem.

PROPOSED SOLUTION

We determine the alignment statistics of two objects by combining geometrical information with position and orientation or pose descriptions. The spatial alignment of two mating objects, O and O′, is depicted in Figure 1. Our treatment of spatial alignment is restricted to cases where it can be represented by the placement of a planar projection of Object O into or on a planar projection of Object O′. A Primed and an Unprimed Cutting Surface are used to create cross-sections of the Objects O and O′ which are then projected onto an Alignment Surface using a Primed and an Unprimed Projection Rule. Both the cross-sections and their relative pose are subject to variation.

The relative pose of the projections is determined with the use of various relative coordinaté transformations. The Alignment Surface is defined by the world coordinate system $X_W Y_W Z_W$. The object fixed coordinate systems $X'_O Y'_O Z'_O$ and $X_O Y_O Z_O$ are used to determine the pose of the objects relative to the world frame. The pose of the cross-sections relative to the object frames is determined using the $X'Y'$ and XY coordinate systems, whereas the pose of the Alignment Surface relative to the world coordinate system is determined using $X_W Y_W$. We restrict our analysis to the case where the cutting and alignment surfaces are parallel planes.

The present work is concerned with objects that have common convex shaped geometries such as lines and circles where closed form solutions are possible. The applicability of using Monte Carlo methods is shown by comparing analytic results to simulation results for the circular case. Results when using complex shapes, where Monte Carlo methods are required, will be given elsewhere. We first present the analysis of placing a line above a second line in order to explain details of the method for a simple case. We then proceed to apply the method to a more practical example of placing a circular geometry, such as that of a pin, on top of a similiar geometry, such as a hole. In both cases a Probability of Successful Assembly function which relates success to geometric and precision parameters is obtained.

ONE-DIMENSIONAL ALIGNMENT ERROR MODEL

The essence of the technique is best described in the one-dimensional case in which a line segment A′B′ is placed on top of another line segment AB as shown in Figure 2. For each trial or sample placement the actual lengths of each line will vary as will their location. In each figure the center of each part is indicated by a tick marker. A satisfactory placement occurs when the bounds of A′B′ are within those of AB as shown in Figure 2-a. An unacceptable placement takes place when either or both sides of A′B′ are exposed as shown in 2-b,c,d.

The actual half lengths LA and LA′ of the line segments, as in Fig. 3, are represented by probability distributions. We assume normal distributions $N(x_{LA};ld,\sigma_{LA})$ and $N(x_{LA'};ld',\sigma_{LA'})$, respectively. Assuming dimensional errors are additive, separation of LA and LA′ into deterministic and stochastic parts results in $LA \doteq ld + DL$, where $DL \sim N(x_{DL};0,\sigma_{LA})$ and $LA' \doteq ld' + DL'$ where $DL' \sim N(x_{DL'};0,\sigma_{LA'})$. The position of the center of each line segment relative to its desired position, F and M, is taken to be $N(x_F;0,\sigma_F)$ and $N(x_M;0,\sigma_M)$, respectively. In practice, the probability distribution of part dimensions and part placements will be determined by sampling and hypothesis testing and the results given in this paper can be so modified. We assume that the distributions of DL, DL′, M and F are statistically independent.

Maximum Allowable Size Ratio, MASR. The Maximum Allowable Size Ratio R, is the largest ratio of ld′ to ld in which A′B′ will fit into AB under the given errors DL, DL′, F and M. The

MASR R for the one-dimensional case is found by noting with the aid of Figure 3 that: the absolute value of the difference between F and M negatively affects the maximum allowable ld′; an increase in the size of the fixtured part AB will allow a larger ld′; and the converse is true for a decreasing manipulated part size A′B′. Thus, the distribution of the MASR is found as

$$R = \frac{\mathrm{ld} + \mathrm{DLL}' - |\mathrm{FTM}|}{\mathrm{ld}} = \frac{\mathrm{ld} + \mathrm{E}}{\mathrm{ld}} = 1 + \frac{\mathrm{E}}{\mathrm{ld}} \tag{1}$$

where $\mathrm{DLL}' \doteq \mathrm{DL} - \mathrm{DL}'$ and $\mathrm{FTM} \doteq \mathrm{F} - \mathrm{M}$. DLL′ and FTM are distributed $N(x_{DLL'};0,\sigma_{DLL'})$ and $N(x_{FM};0,\sigma_{FM}=\sqrt{\sigma_F^2+\sigma_M^2})$, respectively, where $\sigma_{DLL'}=\sqrt{\sigma_{LA}^2+\sigma_{LA'}^2}$ and $\sigma_{FM}=\sqrt{\sigma_F^2+\sigma_M^2}$ [17]. E, the alignment error, is the difference between DLL′ and FM where $\mathrm{FM} \doteq |\mathrm{FTM}|$.

The probability density function (pdf) of FM in the interval $[0,+\infty)$ is

$$f_{FM}(x_{FM}) = \frac{2}{\sigma_{FM}\sqrt{2\pi}}\, e^{-\frac{1}{2}\left(\frac{x_{FM}}{\sigma_{FM}}\right)^2}.$$

The pdf of E in the interval $(-\infty,+\infty)$ under the assumption of statistical independence, is found by convolving the pdfs of DLL′ and FM as

$$f_E(x_E) = \frac{1}{\sqrt{2\pi}\sqrt{\sigma_{FM}^2+\sigma_{DLL'}^2}}\, e^{-\frac{x_E^2}{2(\sigma_{DLL'}^2+\sigma_{FM}^2)}}\, \mathrm{erfc}\left(\frac{1}{\sqrt{2}}\,\frac{\sigma_{FM}}{\sigma_{DLL'}\sqrt{\sigma_{DLL'}^2+\sigma_{FM}^2}}\,x_E\right). \tag{2}$$

The MASR R is described by the pdf $f_R(x_R)$. It is obtained by substituting x_R-1 for x_E in Equation 2 and rescaling the standard deviations by 1/ld. Figure 4 shows the plots of MASR pdfs for various parameter values.

The area under the MASR pdf curve to the right of a given size ratio r provides us with the Probability of Successful Assembly, PSA, of the mating parts if that ratio r of ld$'$ to ld is selected. This probability is expressed as

$$PSA(r) = \int_{r}^{\infty} f_R(x_R) \; dx_R \,. \tag{3}$$

The PSA curves obtained using Gauss-Legendre quadrature based on the pdfs shown in Figure 4 are illustrated in Figure 5. For a given size ratio smaller tolerances and precisions will result in steeper curves at higher probabilities. PSA values larger than zero occur for size ratios above one because there will be some members of the AB and A$'$B$'$ populations that satisfy our acceptance criteria. As tolerances increase the extension of the curves beyond a size ratio of one increases further because there is a larger overlap between the distribution of sizes.

The non-dimensional tolerance variables DL/ld and DL$'$/ld and precision variables F/dl and M/dl provide a natural way of expressing tolerances and precisions. Together with the MASR R, they constitute the parameters of the generic alignment problem. Non-dimensional tolerances and precisions recognize that there is a proportionality in achieving tolerances at a particular size due to material, fabrication and temperature. For example, the probability of successfully placing a 9.99±.02 mm line on a 10.00±.02 mm line with equipment precision of ±.05 mm is identical to that of placing a 99.9±.2 mm line on a 100.0±.2 mm line with equipment precision of ±.5 mm.

Distribution Assumptions. Distribution assumptions other than the normal distribution could be made for the tolerance and/or precision errors. A uniform distribution assumption would be safer in the case where we do not have any information about the distribution of the errors. In addition, some of the error factors in our model may prove to be insignificant and could thus be eliminated. For example, when tolerance errors are normal, there are no fixturing errors, and the manipulator precision is uniform in $[-\frac{R}{2},+\frac{R}{2}]$, application of the above method will yield:

$$f_E(x_E) = \frac{1}{2R}\left\{\mathrm{erfc}\left(\frac{x_E}{\sqrt{2}\sigma_{DLL'}}\right) - \mathrm{erfc}\left(\frac{R+x_E}{\sqrt{2}\sigma_{DLL'}}\right)\right\}.$$

TWO-DIMENSIONAL ALIGNMENT ERROR MODELS

Error Vectors and Probability Density Functions. A vectoral representation of tolerances and placement errors will allow the generalization of the above-illustrated theory for point symmetrical two-dimensional geometries. For each of the two mating parts the points of symmetry are mapped into point O_1, the origin of the precision coordinate system as shown in Figure 6. The positioning errors of the manipulator and the fixture with respect to the origin are represented by the random vectors F and M, respectively. The positioning error of the manipulator with respect to the fixture is thus FTM $\doteq$ F - M. The success of the assembly is a function of the magnitude of FTM , FM. A one-dimensional tolerance coordinate system is placed at the tip of FTM with positive direction in the direction of FTM. The tolerance coordinate is aligned with FTM because in point symmetrical perfect form objects the contact between the parts occurs only in the direction of FTM. When FTM = 0, the contours of the objects will come in full contact and the tolerance direction can be specified arbitrarily. The total tolerance error of the manipulated and fixtured parts is given by $DLL' \doteq DL - DL'$. Generalization of Equation 1 yields

$$R = \frac{ld + s\,|DLL'| - |FTM|}{ld} \tag{4}$$

where,

$$s = \begin{cases} +1 \text{ if } DLL' \text{ has } (+) \text{ direction} \\ -1 \text{ if } DLL' \text{ has } (-) \text{ direction} \end{cases}$$

In the one-dimensional case Equation (4) reduces to:

$$R = \frac{ld + DL - DL' - |F - M|}{ld}; \tag{5.a}$$

while in the two-dimensional case it becomes:

$$R = \frac{ld + DL - DL' - \sqrt{(X_F - X_M)^2 + (Y_F - Y_M)^2}}{ld}. \tag{5.b}$$

where $\sqrt{(X_F-X_M)^2+(Y_F-Y_M)^2}$ has been substituted for $|F-M|$. The geometric interpretation for these variables is given in Figure 7.

We derive the alignment error pdfs here for the correlated and uncorrelated cases in a manner similar to that used in the one-dimensional case presented above. The two-dimensional precision errors are represented by bivariate distributions; in the one-dimensional model they were half normal. In a bivariate precision error distribution, correlations among the components of the random precision vectors $F=(X_F,Y_F)'$ and $M=(X_M,Y_M)'$ are taken into account.

The distributions of the independent normal vectors $(X_F,Y_F)'$ and $(X_M, Y_M)'$ are:

$$f_F(F) = \frac{1}{2\pi\sqrt{\det(C_F)}} e^{-\frac{1}{2}F' C_F^{-1} F}$$

$$f_M(M) = \frac{1}{2\pi\sqrt{\det(C_M)}} e^{-\frac{1}{2}M' C_M^{-1} M}$$

where $f_M(M)$ and $f_F(F)$ are the manipulator and fixture precision error pdfs with covariance matrices C_M and C_F, respectively.

The covariance matrix of a random vector $(X,Y)'$ is denoted by

$$C_{xy} = \begin{bmatrix} \sigma_{xx} & \sigma_{xy} \\ \sigma_{yx} & \sigma_{yy} \end{bmatrix}$$

where σ_{xx} and σ_{yy} represent the variances measured along the x- and y-axes; $\sigma_{xy}=\sigma_{yx}$ is the covariance between X and Y. It is customary to write σ_{xx} and σ_{yy} as σ_x^2 and σ_y^2, respectively and replace σ_{xy} and σ_{yx} with $\rho\sigma_x\sigma_y$, where $-1\leq\rho\leq 1$ is the correlation coefficient of the random variables X and Y.

Correlated Precision Errors. We determine the pdf $f_{FM}(x_{FM})$ by first noting the random variable FM is a function of the random variables U and V where $U \doteq X_F - X_M$ and $V \doteq Y_F - Y_M$ such that $FM \doteq \sqrt{U^2+V^2}$. The joint distribution of U and V is $N(x_U, x_V; 0, 0, \sqrt{\sigma_{XF}^2+\sigma_{XM}^2}, \sqrt{\sigma_{YF}^2+\sigma_{YM}^2}, \rho_{uv})$ where

$$\rho_{uv} = \frac{\rho_F\sigma_{XF}\sigma_{YF}+\rho_M\sigma_{XM}\sigma_{YM}}{\sqrt{\sigma_{XF}^2+\sigma_{XM}^2}\sqrt{\sigma_{YF}^2+\sigma_{YM}^2}}.$$

Using the transformations $x_U = x_{FM}\cos\delta$ and $x_V = x_{FM}\sin\delta$ we write $f_{FM\delta}(x_{FM},\delta) = f_{UV}(x_U,x_V)|J|$ where J is the Jacobian of the transformation. Integrating $f_{FM\delta}(x_{FM},\delta)$ with respect to δ from 0 to 2π, we obtain the pdf:

$$f_{FM}(x_{FM}) = \frac{x_{FM}}{\sigma_U\ \sigma_V\ \sqrt{(1-\rho_{uv}^2)}}\ e^{-\frac{1}{4}\frac{\sigma_U^2+\sigma_V^2}{\sigma_U^2\sigma_V^2(1-\rho_{uv}^2)}x_{FM}^2}\ \sum_{n=0}^{\infty}\frac{(A^2+B^2)^n}{(2n)^2!}$$

where $A = -\frac{1}{4}\frac{\sigma_U^2-\sigma_V^2}{\sigma_U^2\sigma_V^2(1-\rho_{uv}^2)}x_{FM}^2$ and $B = \frac{1}{2}\frac{\rho_{uv}}{\sigma_U\sigma_V(1-\rho_{uv}^2)}x_{FM}^2$.

The pdf for the alignment error E , $f_E(x_E)$, where $x_E = x_{DLL'} - x_{FM}$, is then obtained by convolving the tolerance distribution of $DLL' \sim N(x;0,\sigma_{DLL'}=\sqrt{\sigma_{LA}^2+\sigma_{LA'}^2})$ with $f_{FM}(x_{FM})$.

The pdf of the MASR, $f_R(x_R)$, is obtained by substituting x_R-1 for x_E and rescaling the standard deviations by 1/ld in $f_E(x_E)$. The PSA is obtained by integrating $f_R(x_R)$ from a given size ratio r to ∞.

Uncorrelated Precision Errors With Equal Variances. In this case U and V are independently normally distributed variables with mean 0 and variance $\sigma_{FM}^2 = \sigma_{XF}^2 + \sigma_{XM}^2 = \sigma_{YF}^2 + \sigma_{YM}^2$. The random variable FM will thus have a Rayleigh distribution:

$$f_{FM}(x_{FM}) = \frac{x_{FM}}{\sigma_{FM}^2}\ e^{-\frac{1}{2}\left(\frac{x_{FM}}{\sigma_{FM}}\right)^2}$$

defined in the interval $[0,+\infty)$. The pdf for the alignment error E becomes

$$f_E(x_E) = -\frac{\sigma_{FM}}{2(\sigma_{FM}^2+\sigma_{DLL'}^2)^{3/2}} e^{-\frac{x_E^2}{2(\sigma_{DLL'}^2+\sigma_{FM}^2)}} \operatorname{erfc}\left(\frac{1}{\sqrt{2}} \frac{\sigma_{FM}}{\sigma_{DLL'}\sqrt{\sigma_{DLL'}^2+\sigma_{FM}^2}} x_E\right) x_E$$

$$+ \frac{\sigma_{DLL'}}{\sqrt{2\pi}\,(\sigma_{FM}^2+\sigma_{DLL'}^2)} e^{-\frac{x_E^2}{2\,\sigma_{DLL'}^2}}$$

To obtain $f_R(x_R)$, x_E is replaced by x_R-1 and the standard deviations are scaled by 1/ld. The PSA is obtained by integrating $f_R\ (x_R)$ from a given size ratio r to ∞.

VERIFICATION AND MONTE CARLO SIMULATION

The equations for the PSA developed in this paper, for the one dimensional case (Equation 5a) and the two dimensional cases (Equation 5b) with and without correlation have been verified using Monte Carlo simulations of the assembly process. The simulation procedure consists of 1) generating a set of random deviates for the variables in the error model equation, 2) computing a MASR using the error model equation (Equation 5a or 5b), 3) repeating Steps 1 and 2 until a "sufficiently" large number n of MASR values $R_1, \dots, R_n$ is computed, 4) sorting the computed MASRs from the smallest $R^{(1)}$ to the largest $R^{(n)}$, and 5) plotting $\frac{n+1-i}{n}$ versus $R^{(i)}$. The PSA using this method will vary from 1/n to 1 [18].

Figure 8 compares the result of using a Monte-Carlo simulation, with n=1000, with that of using the analytical method described above for the uncorrelated two dimensional assembly. Despite the low number of observations, Monte Carlo simulation result appears to be in close agreement with the analytical solution and will be found to be a powerful technique for the implementation of the proposed method when analyzing complex geometries, the subject of a future paper.

APPLICATIONS

The equations developed above can be used directly to estimate the Probability of Successful Assembly for given size ratio, tolerance and precision values. They must be used iteratively to select part dimensions and tolerances given the precision of the equipment and the required assembly performance. As an aid to this iterative approach design surfaces and tables can be used.

DESIGN SURFACES

The MASR that would provide a certain level of PSA can be plotted for various combinations of equipment precision and part tolerances. For example, Figure 9 shows the effect of assuming equal tolerances for the manipulated and fixtured parts and equal precisions for the manipulator and fixture when the probability of successful assembly is .99 in the two-dimensional uncorrelated model. We define a tolerance or precision level, which is used in scaling the axes of the surface graph, as the negative common logarithm of their values. An infinite combination of tolerances and precisions can be used to achieve the desired PSA for this and any other particular size ratio. The dashed line is a surface contour for the tolerances and precision that would give a PSA of .99 for a size ratio of .9.

The surface in Figure 9 is not symmetrical with respect to tolerance and precision. Optimal precision and tolerances can be chosen based on their costs and the costs associated with failure of the assembly process. Let us assume that the cost of failure of the assembly process requires that a PSA of .99 be achieved. Let us also assume that the costs for achieving a particular level of precision and tolerance are equal and the cost is proportional to its level [19]. Under these special conditions the non-dimensional tolerances and precisions should be selected so that the equipment precision is slightly better than the part tolerance because of the asymmetry of the surface. We are currently developing a model for cost optimal selection of the equipment precision, part tolerances and size ratios to cover other sets of conditions.

Figure 9 represents the design surface for a particular PSA value. We obtain an onion skin like grouping of surfaces by varying the PSA value. A cut through the set of surfaces at PSAs of .9, .99 and .999 along the equal tolerance/precision plane results in Figure 10. We see from this figure the obvious conclusions that; to achieve a higher PSA, for any particular size ratio, requires higher precision and tolerance levels and that; for any particular tolerance and precision level the PSA can be increased by simply reducing the size ratio. The exact effect of these changes can be determined by presentation of the surfaces in tabular form.

DESIGN TABLES

Tables of MASRs can be obtained using either Monte Carlo methods or the analytical technique presented above. Table I-b corresponds to the surface given in Figure 9 whereas Tables I-a and I-c are for surfaces at PSAs of .9 and .999, respectively. Figure 10 is provided by the diagonal terms of the three tables. The tables have been so constructed that linear interpolation can be used to determine one of the size ratio, precision and tolerance levels given the other two.

The ability to use a larger MASR to achieve a particular PSA in many cases allows the assembly to function at a higher capability. This is because the mechanical function of many assemblies degrades with the magnitude of the clearance. The rows of the tables show that increasing the precision level increases the maximum size ratio allowed when achieving the desired PSA level. Similarly the columns show that increasing the tolerance level increases the maximum size ratio allowed when achieving the desired PSA level.

Increasing the tolerance or precision levels into either the upper right or lower left hand corners of the table does not significantly increase the size ratio allowed. Conversely, assuming that the cost of tolerances and precisions is proportional to their level, combinations of tolerances and precisions within these regions will significantly increase production costs without measurable improvement in the function of the assembly. The size ratios do not differ significantly indicating unnecessarily precise equipment or part tolerances.

If a designer chooses to insert a nominally 19.97 mm radius pin into a 20.00 mm radius hole various assembly performances are achieved depending on the tolerance specifications of the hole and pin. Let us assume that we are using equipment with a precision level of three. This is represented by the fifth column of Tables I-a, b and c. When using a size ratio of $.9985 = 19.97/20.00$ the tables indicate that to achieve a PSA of .9, a minimum nominal part tolerance of $\pm(20\ \text{mm})\times 10^{-2.928} \simeq \pm .02$ mm is required. To achieve a PSA of .99 a minimum nominal part tolerance of $\pm(20\ \text{mm})\times 10^{-3.5} \simeq \pm .006$ mm is required. And, to achieve a PSA of .999 is impossible. Selecting equipment with precision level 3.5 would make a PSA of .999 possible. The exponents in the parentheses are obtained by linear interpolations. The designer and the machine shop must then determine the cost benefits of each of these possibilities in order to make the appropriate selection.

CONCLUSION

The concerns of the design department and the fabrication shop are unified in an assembly performance model which combines the effects of the part dimensions and tolerances and the equipment precision in the Probability of Successful Assembly, PSA. The probability of achieving a successful alignment when using parts with a given size ratio, tolerance and equipment precision is given by the PSA. Various probability distributions associated with the manufacturing and assembly processes can be used.

The PSA also provides a way of determining the part dimensions and tolerances when using equipment with a given precision when the maximum allowable assembly failure rates are known. When used in this manner MASR Tables provide the MASR that can be used to achieve the required level of success.

The methodology exposed in this paper for the alignment of line segments and circles can be extended to more complex shapes including the alignment of single and multiple paired polygons common to the electronic, civil and mechanical industries. Further enhancements include methods for incorporating system compliances in the determination of the effective size ratios and determining cost optimal solutions. In the case of complex geometrical shapes and probability distributions, Monte Carlo simulation appears to be a powerful technique for implementation of the method.

ACKNOWLEDGEMENT

The research described here was supported by Lehigh University's Engineering Research Center for Advanced Technology for Large Structural Systems with funding from National Science Foundation Cooperative Aggrement ECD-8943455. Any opinions, findings, conclusions, or recommendations expressed in this publication are those of the authors and do not necessarily reflect the views of the National Science Foundation.

REFERENCES

[1] Abdel-Malek, Layek, "A Case Study on the Use of Robots in Assembly Processes," Engineering Costs and Production Economics, No.9, 1985.

[2] Lozano-Perez, T., et al., "Automatic Synthesis of Fine- Motion Strategies for Robots," The International Journal of Robot ics Research, Vol.1, No.1, Spring 1984.

[3] Whitney, D. E., "Force Feed-Back Control of Manipulator Fine Motions," Journal of Dynamic Systems, Measurement and Control, Vol.1 , March 1982.

[4] Laktianov, N. M. and Andreev, G. Ya., "The Automatic Assembly of Parts," Russian Engineering Journal, Vol. XLVI, No.8, 1966.

[5] Whitney, E. D., et al., "Designing Chamfers," The International Journal of Robotics Research, Vol.2, No.4, Winter 1983.

[6] Nevins, J. L. and Whitney, D. E., "Computer-controlled Assembly," Scientific American, February 1978.

[7] U.S. Patent, No. 4,098,001, Watson, P. C., "Remote Center Compliance System," 4 July 1978, and U.S. Patent No. 4,155,169, Drake, S. H. and Simunovich, S. N., "Compliant Assembly Device," May 22, 1979.

[8] Watson, P. C., "Instrumented Remote Center Compliance," U. S. Patent No. 4,316,319, issued February 23, 1982, filed September19, 1979.

[9] Hasegawa, H., and Sakata, T., "Non-Contact Precision Insertion Technique," Proceedings of the 6th International Conference on Assembly Automation, 15-17 May 1985, Birmingham, UK.

[10] Quick, Joseph H., et al, Work-Factor Time Standards, McGraw-Hill, 1962.

[11] Coley, David. P., "Instant Prototypes," Mechanical Engineering, Vol.110, No.7, July 1988.

[12] Abdul-Malek, Layek and Boucher, Thomas O., "A Framework for the Economic Evaluation of Production System and Product Design Alternatives for Robot Assembly," International Journal of Production Research, 1985, Vol. 23, No.1.

[13] Abdul-Malek, Layek, "A Framework for the Robotic Assembly of Parts with General

Table 1. MASR Tables for 2-D Alignment; Uncorrelated

a) PSA = .9

$-\text{Log}_{10}$(Bilat. Spec. Precision)

$-\text{Log}_{10}$(Bilat. Spec. Tolerance)	1	1.5	2	2.5	3	3.5	4	4.5	5
1	* 0.87	0.92	0.93	0.94	* 0.94	0.94	0.94	0.94	0.94
1.5	* 0.90	0.957	0.973	0.980	* 0.980	0.980	0.980	0.980	0.980
2	* 0.90	* 0.967	0.987	0.992	0.993	0.994	* 0.994	0.994	0.994
2.5	* 0.90	0.967	* 0.990	0.9957	0.9973	0.9980	* 0.9980	0.9980	0.9980
3	* 0.90	0.967	0.990	* 0.9967	0.9987	0.9992	0.9993	0.9994	* 0.9994
3.5	* 0.90	0.967	0.990	0.9967	* 0.9990	0.99957	0.99973	0.99980	* 0.99980
4	* 0.90	0.967	0.990	0.9967	0.9990	* 0.99967	0.99987	0.99992	0.99993
4.5	* 0.90	0.967	0.990	0.9967	0.9990	0.99967	* 0.99990	0.999957	0.999973
5	* 0.90	0.967	0.990	0.9967	0.9990	0.99967	0.99990	* 0.999967	0.999987

b) PSA = .99

$-\text{Log}_{10}$(Bilat. Spec. Precision)

$-\text{Log}_{10}$(Bilat. Spec. Tolerance)	1	1.5	2	2.5	3	3.5	4	4.5	5
1	* 0.81	0.87	0.88	0.89	* 0.89	0.89	0.89	0.89	0.89
1.5	* 0.85	0.940	0.957	0.963	0.963	0.967	* 0.967	0.967	0.967
2	* 0.86	0.953	0.981	0.987	0.988	0.989	* 0.989	0.989	0.989
2.5	* 0.86	0.953	* 0.985	0.9937	0.9957	0.9963	0.9963	0.9967	* 0.9967
3	* 0.86	0.953	* 0.986	0.9953	0.9981	0.9987	0.9988	0.9989	* 0.9989
3.5	* 0.86	0.953	0.986	0.9953	* 0.9985	0.99937	0.99957	0.99963	* 0.99963
4	* 0.86	0.953	0.986	0.9953	* 0.9986	0.99953	0.99980	0.99987	0.99988
4.5	* 0.86	0.953	0.986	0.9953	0.9986	0.99953	* 0.99985	0.999937	0.999960
5	* 0.86	0.953	0.986	0.9953	0.9986	0.99953	* 0.99986	0.999953	0.999980

c) PSA = .999

$-\text{Log}_{10}$(Bilat. Spec. Precision)

$-\text{Log}_{10}$(Bilat. Spec. Tolerance)	1	1.5	2	2.5	3	3.5	4	4.5	5
1	* 0.79	0.85	* 0.85	0.85	0.85	0.85	0.85	0.85	0.85
1.5	* 0.83	0.927	0.950	0.953	* 0.953	0.953	0.953	0.953	0.953
2	* 0.83	* 0.943	0.977	0.983	0.985	* 0.985	0.985	0.985	0.985
2.5	* 0.83	0.943	* 0.982	0.9923	0.9947	0.9953	* 0.9953	0.9953	0.9953
3	* 0.83	0.943	* 0.983	0.9943	0.9976	0.9983	0.9985	* 0.9985	0.9985
3.5	* 0.83	0.943	0.983	0.9943	* 0.9982	0.99923	0.99947	0.99953	* 0.99953
4	* 0.83	0.943	0.983	0.9943	0.9982	* 0.99943	0.99976	0.99983	0.99985
4.5	* 0.83	0.943	0.983	0.9943	0.9982	0.99943	* 0.99982	0.999923	0.999947
5	* 0.83	0.943	0.983	0.9943	0.9982	0.99943	0.99982	* 0.999943	0.999976

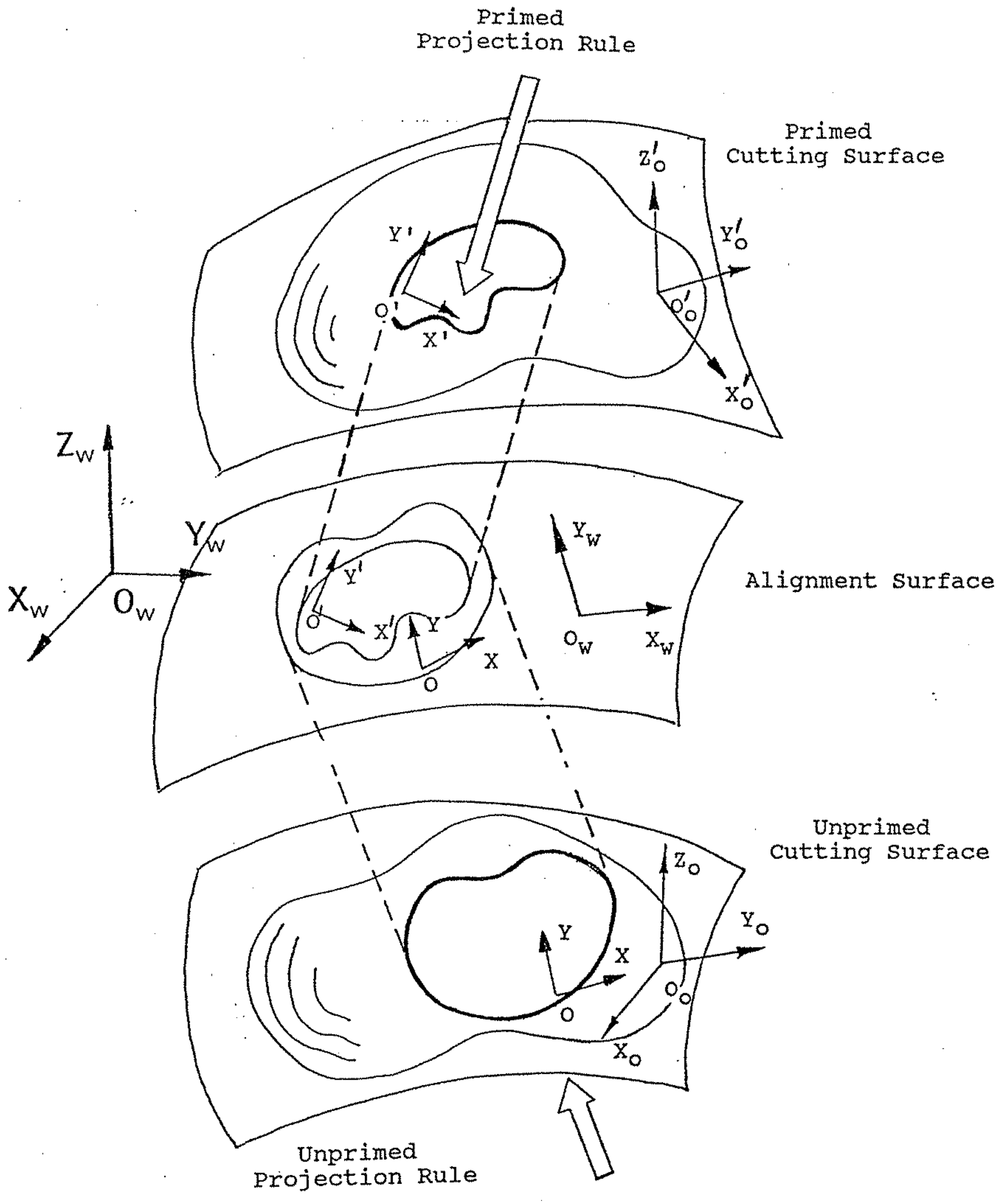

Figure 1. Planar Alignment of Two 3-D Objects

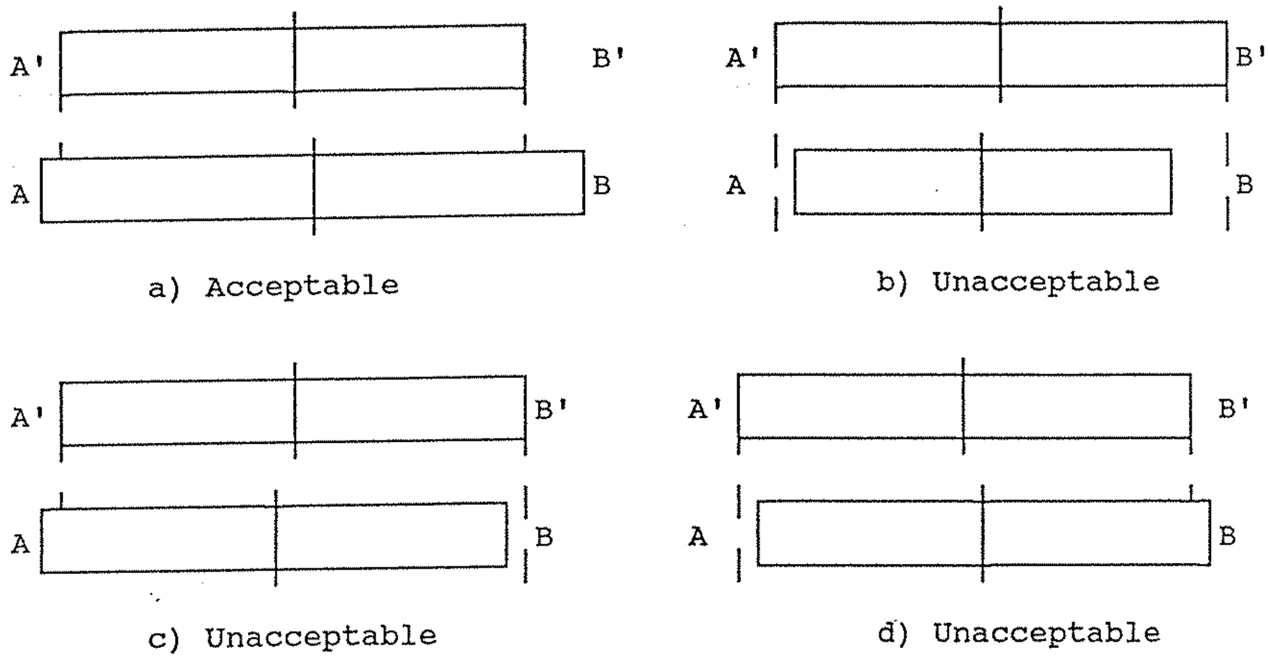

Figure 2. Acceptable and Unacceptable Alignment Modes

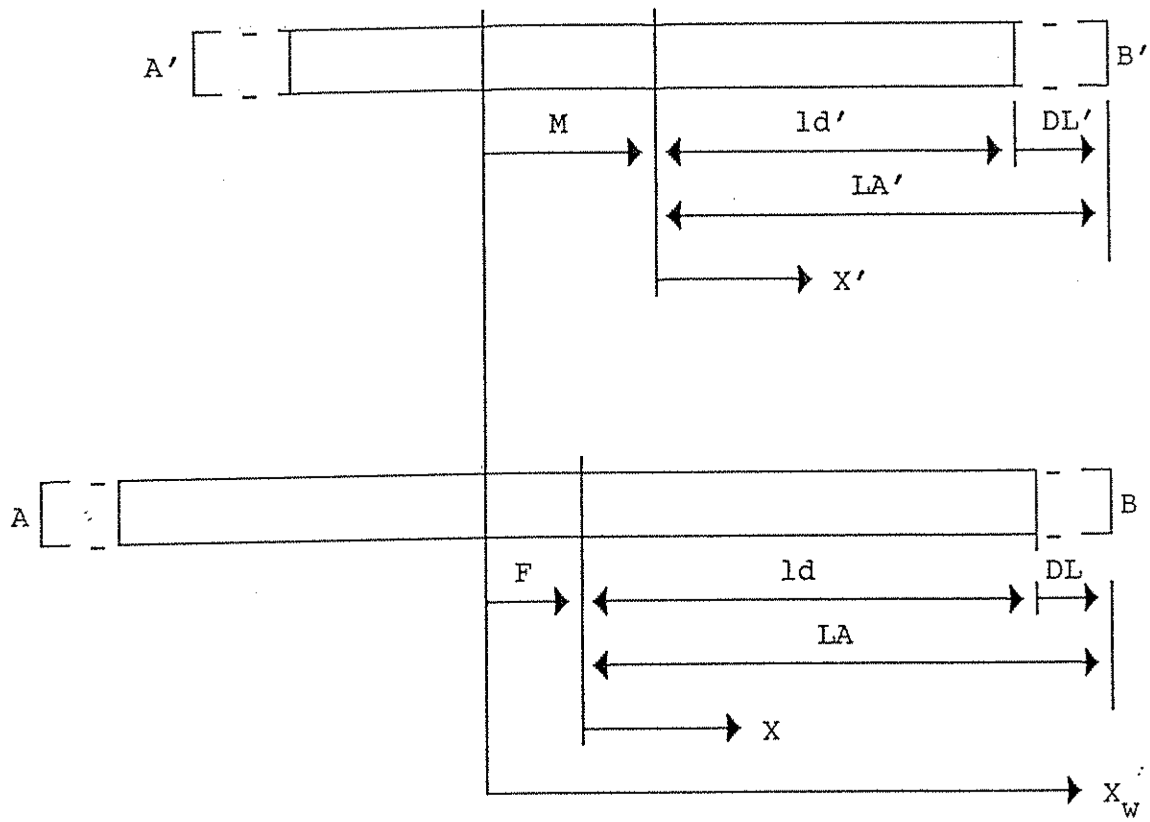

Figure 3. 1-D Alignment Error Model

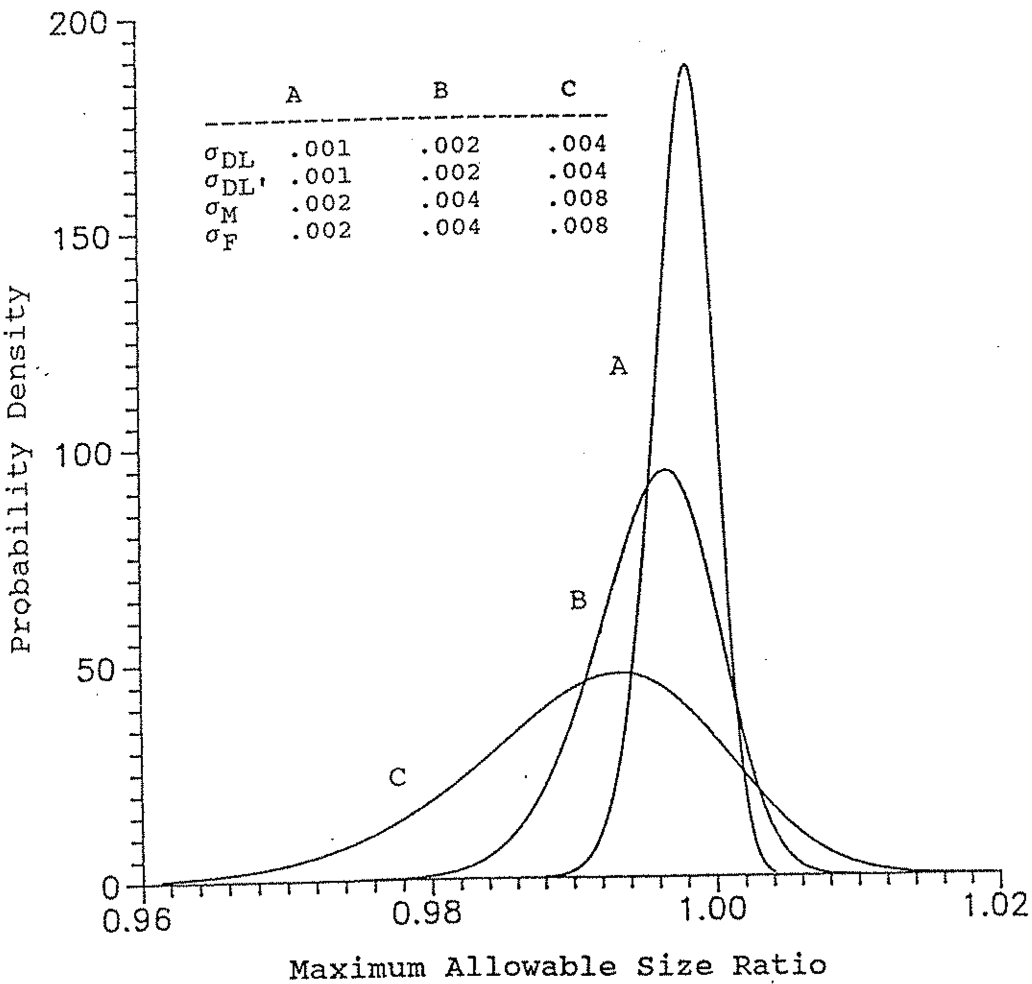

Figure 4. Probability Density Function for 1-D Alignment

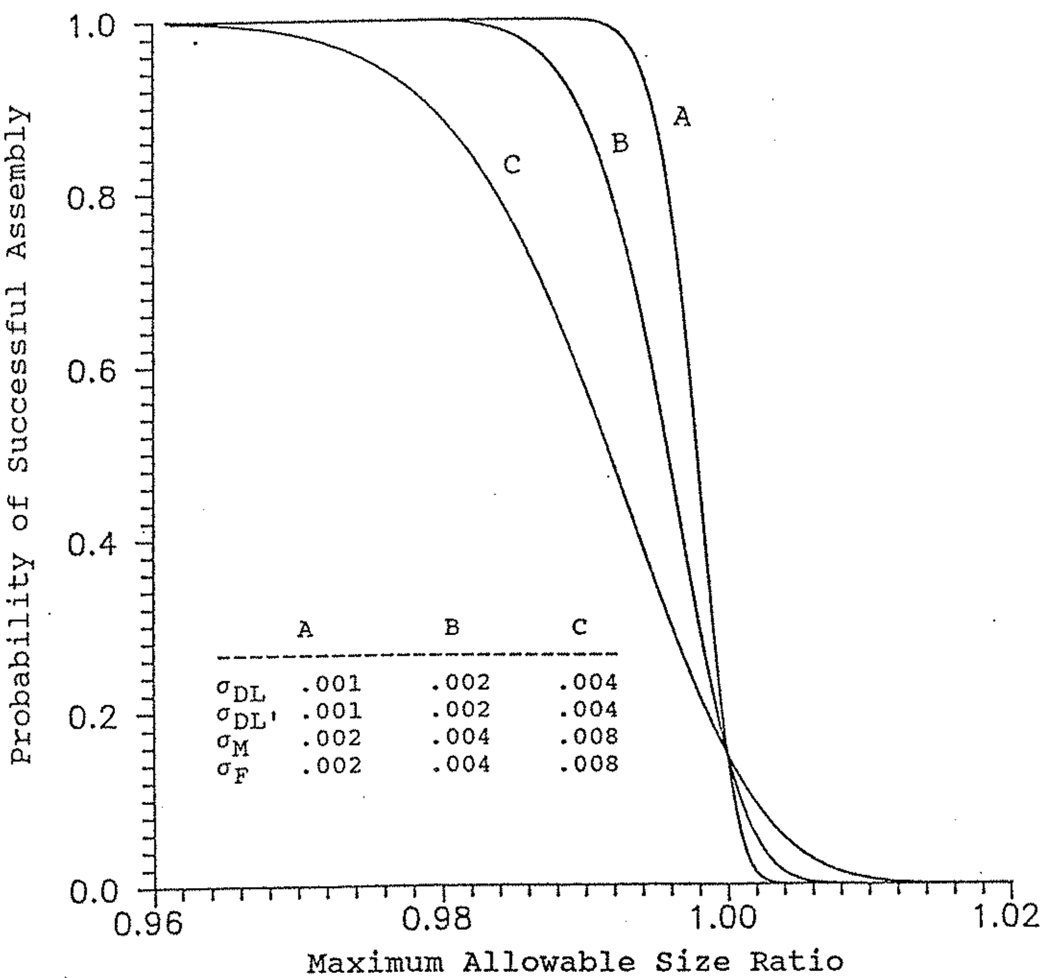

	A	B	C
σ_{DL}	.001	.002	.004
$\sigma_{DL'}$	.001	.002	.004
σ_M	.002	.004	.008
σ_F	.002	.004	.008

Figure 5. Probability of Successful Assembly Curves for 1-D Alignment

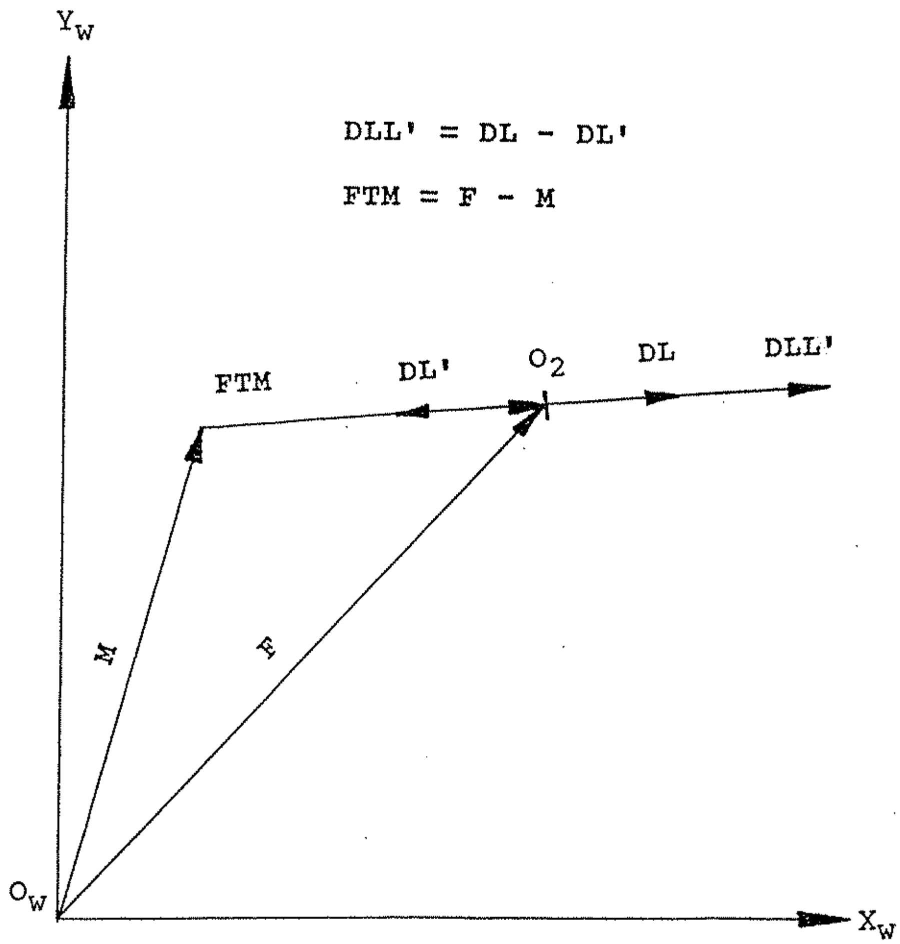

Figure 6. Vectoral Representation of Tolerances and Precisions

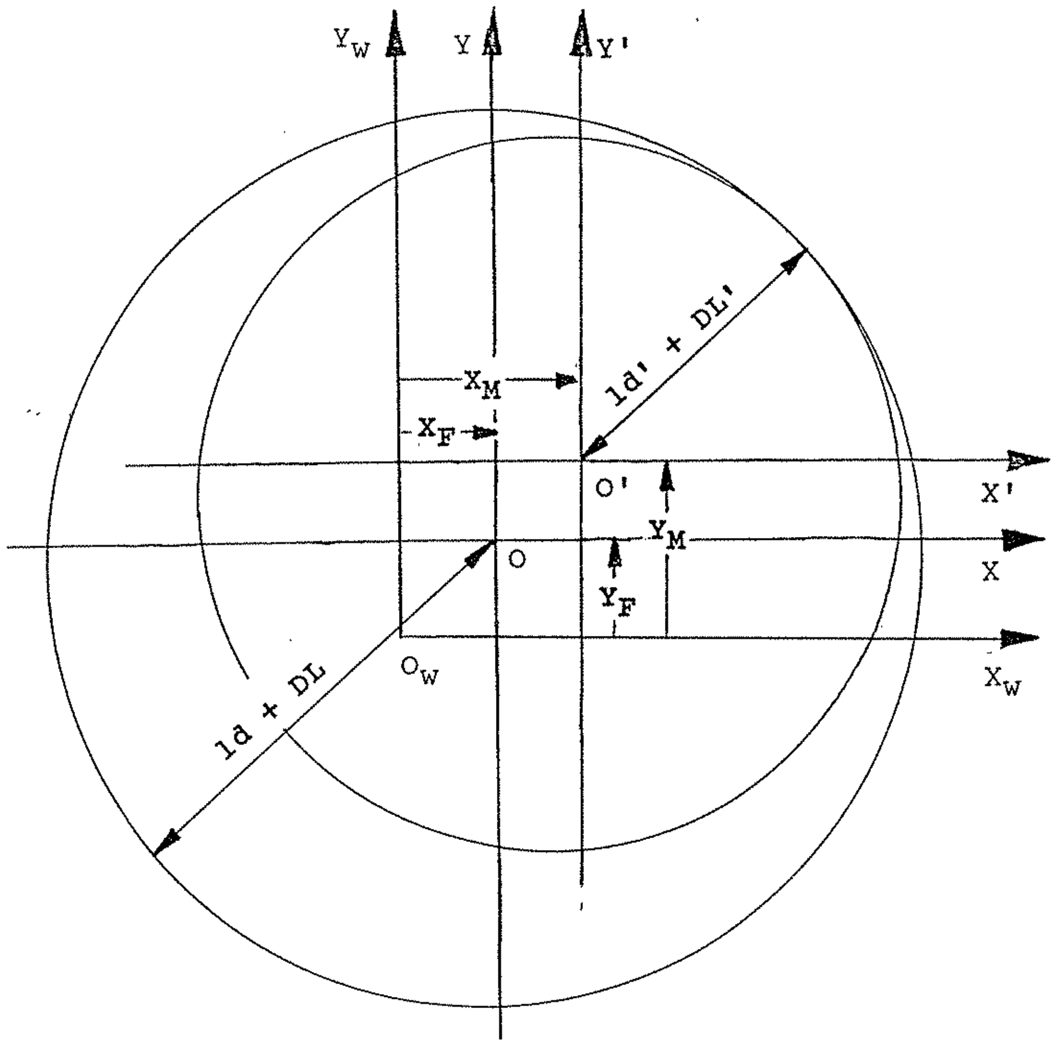

Figure 7. 2-D Alignment Error Model

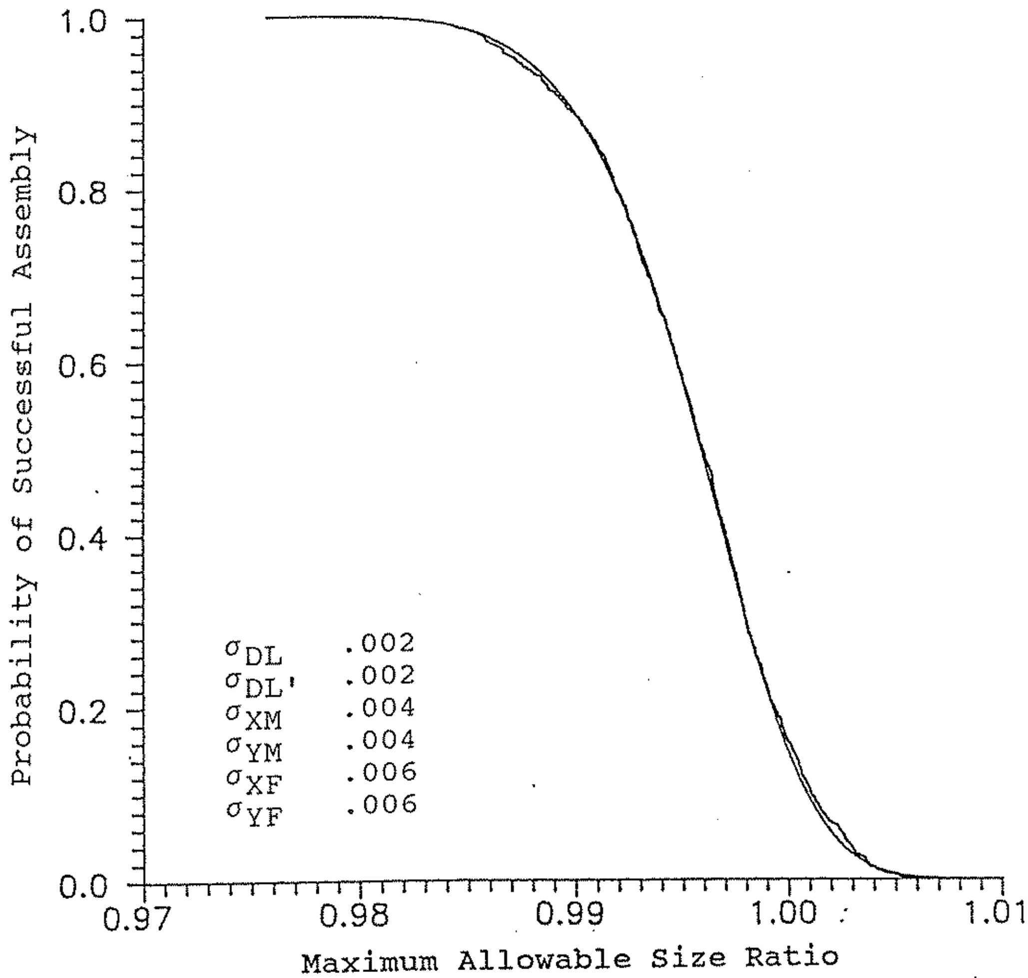

Figure 8. Monte Carlo Simulation and Analytical Solution for 2-D Alignment; Uncorrelated

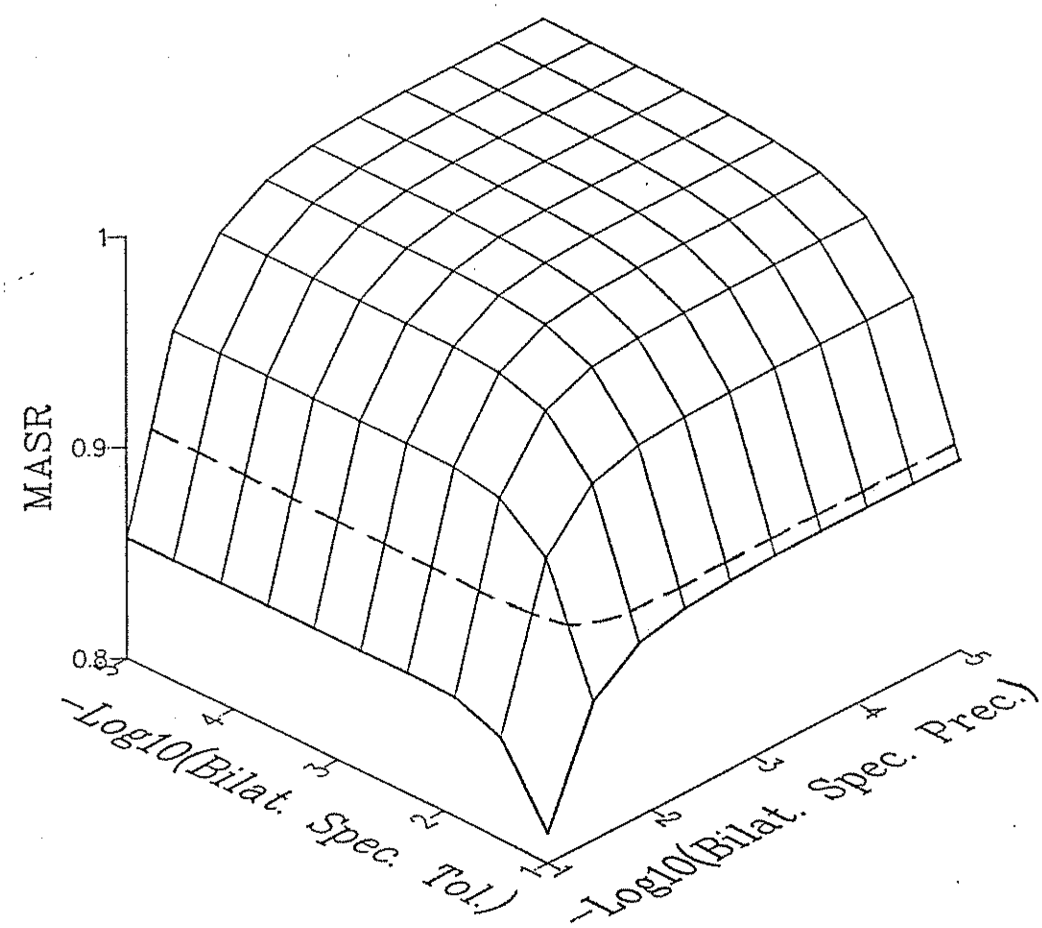

Figure 9. Design Surface for 2-D Alignment with PSA=.99; Uncorrelated

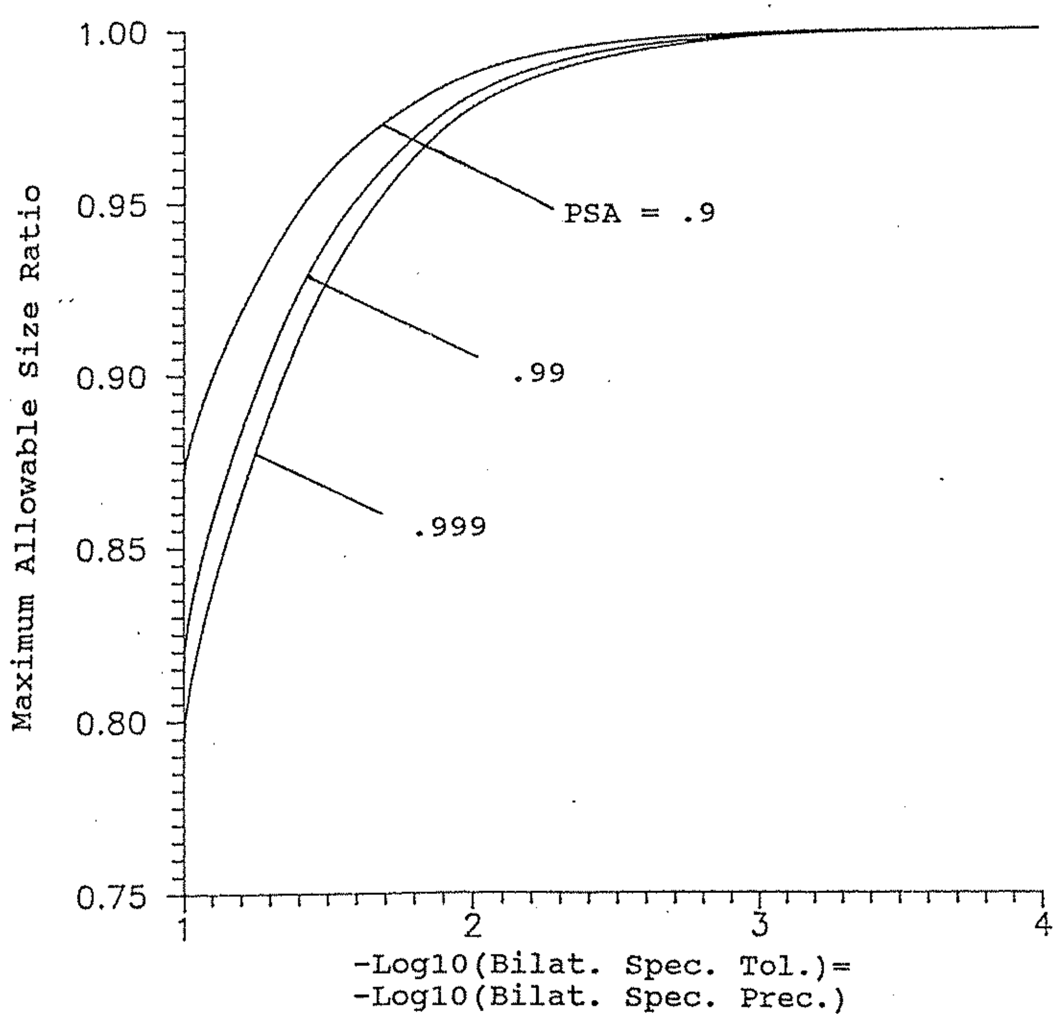

Figure 10. MASR vs Equal Tolerance and Precision for 2-D Alignment; Uncorrelated